

Multiple light scattering in multilayered media: theory, experiments

A. da Silva^{a,*}, C. Andraud^a, E. Charron^a, B. Stout^b, J. Lafait^a

^aLaboratoire d'Optique des Solides, Université Paris 6 UMR CNRS 7601-Case 80-4, Place Jussieu, 75252 Paris cedex 05, France

^bInstitut Fresnel, Faculté des Sciences et Techniques, Centre de Saint Jérôme-UMR 6133, 13397 Marseille cedex 20, France

Abstract

The model presented here is based on the resolution of the radiative transfer equation, by the Discrete Ordinate Method, in the steady-state domain. A matricial formulation leads to the resolution of the problem of light scattering through multislabs, with index mismatch at each interface. In that way, the angular distribution of out-going fluxes is obtained. A complete dissociation between volume and interfaces behaviors allows the introduction of elaborated theories to describe them properly. An analytical scattering theory based on the T-matrix formalism is introduced to account for interactions between scatterers, when high volume fractions are considered. Theoretical calculations are compared with experiments obtained with a spectro-scatterometer.

© 2003 Elsevier B.V. All rights reserved.

Keywords: Light scattering; Radiative transfer theory; Discrete ordinate method; T-matrix method

1. Introduction

Optical properties of media scattering and absorbing light and their calculation are problems of interest in many disciplines. When weak scatterers volume fractions are considered, these properties are commonly calculated by solving the radiative transfer equation (RTE) [1]. As this equation supposes no electromagnetic interactions between scatterers, for high volume fractions, an exact calculation accounting for interactions between fields scattered by all particles is to be performed. Even if it can theoretically be made, the techniques usually developed are time consuming, and become non-realistic for high optical

thickness. As a first step, to account for dependent multiple light scattering phenomenon in dense media, we suggest a two-fold approach: (i) we define a coherence volume in which we carry an exact calculation of the scattering parameters (extinction, scattering cross sections and phase function for the set of particles), using Analytical Scattering Theory (AST) [2,3], based on a T-matrix method [4], (ii) these parameters are then introduced in the RTE, and macroscopic optical properties (reflected and transmitted angular distribution of flux) are then determined. In the second section of this paper, we briefly present the theoretical models used. We chose to solve RTE by using the Discrete Ordinate Method (DOM) [1]. The treatment has been extended to a multiple slab formulation, by dissociating volume scattering behavior from interfaces and using a matrix

*Corresponding author. Fax: 00-33-1-44-27-39-82.

E-mail address: adasilva@ccr.jussieu.fr (A. da Silva).

formulation. In Section 3, we describe an experimental device (spectro-scatterometer) especially designed for validation of the theoretical model. We performed experiments on gauged media such as latex beads in water. The results are presented and commented in Section 4.

2. Theories

2.1. Radiative transfer equation

The RTE stems from an energy balance and describes the spatio-temporal evolution of flux \mathbf{F} at a point \mathbf{r} and in direction \mathbf{u} . Experiments were performed for steady-state case, for slab geometry and under non-polarized normal illumination. \mathbf{F} depends only on z and the scattering detection direction $\mu = \cos \theta$. If $\mathbf{F}(z, \mu)$ denotes the total flux, at depth z in the medium and scattered in the direction μ :

$$\begin{aligned} & \underbrace{\frac{\partial \mathbf{F}(z, \mu)}{\partial z}}_{\text{flux variation in element } dz} \\ &= - \underbrace{\frac{\mathbf{k}_{\text{ext}}}{\mu} \mathbf{F}(z, \mu)}_{\text{loss by scattering and absorption in direction } \mu} \\ &+ \underbrace{\mathbf{k}_{\text{sca}} \int_{-1}^1 \frac{\mathbf{F}(z, \mu')}{\mu'} \tilde{\mathbf{p}}(\mu, \mu') d\mu'}_{\text{gain by scattering from all directions } \mu' \text{ towards direction } \mu}. \end{aligned} \quad (1)$$

The properties of the scattering medium are then totally described by: (i) extinction and scattering coefficients (respectively \mathbf{k}_{ext} and \mathbf{k}_{sca}); (ii) the phase function $\tilde{\mathbf{p}}(\mu, \mu')$ representing the probability for a radiation, incident in direction μ' to be scattered in direction μ . In that condition, the integral in Eq. (1) can be efficiently evaluated by DOM, consisting on a spatial discretization into N directions. One can then rewrite (1) with vector notations:

$$\frac{d\mathbf{F}}{dz} = \mathbf{S} \mathbf{F}, \quad S_{ij} = \frac{\mathbf{k}_{\text{sca}}}{\mu_i} \tilde{\mathbf{p}}(\mu_i, \mu_j) \omega_i, \quad S_{ij} = -\frac{\mathbf{k}_{\text{ext}}}{\mu_j}. \quad (2)$$

The general solution of this equation is

$$\mathbf{F}_i = \sum_{\alpha=1}^N A_{i\alpha} C_{\alpha} e^{\lambda_{\alpha} z}, \quad i \in [1, N], \quad (3)$$

where λ_{α} and $A_{i\alpha}$ are respectively the eigenvalues and the eigenvectors of matrix \mathbf{S} . Coefficients C_{α} are weighting coefficients issued from boundary conditions. The easiest way to solve multilayered systems problem is to **uncouple** the behavior of the scattering medium from its interfaces, in order to relate out-going flux \mathbf{F}_{out} directly to incident flux \mathbf{F}_{in} . Let Z be the total thickness of the scattering medium. By applying boundary conditions **inside** the medium ($z = 0^+$ and $z = Z^-$), one can define a “transfer” matrix \mathbf{Q} (see Ref. [5] for expression): $\mathbf{F}_{\text{out}} = \mathbf{Q} \mathbf{F}_{\text{in}}$. It is then shown that the matrix equivalent to a multislabs is nothing than the product of individual \mathbf{Q} matrices of each slab.

2.2. Scattering parameters

As mentioned above, the solutions depend on the extinction and scattering coefficients, $\mathbf{k}_{\text{ext}} = n\sigma_{\text{ext}}$, $\mathbf{k}_{\text{sca}} = n\sigma_{\text{sca}}$, where n is the number of scatterers by unit volume, σ_{ext} and σ_{sca} , are respectively the total extinction and scattering cross sections; and on the phase function integrated over all azimuthal directions:

$$\tilde{\mathbf{p}}(\mu_i, \mu_j) \equiv \int_0^{2\pi} \mathbf{p}(\mathbf{u}_i \cdot \mathbf{u}_j) d\phi. \quad (4)$$

The phase function $\mathbf{p}(\mathbf{u}_i \cdot \mathbf{u}_j)$ is defined [6] as the ratio of the differential scattering cross section to the total scattering cross section. When weak volume fractions are considered, there is no interaction between fields scattered by the particles, and we can deduce the differential and the total cross sections from Mie theory [7] for a single spherical particle. For high volume fractions, electromagnetic interactions have to be taken into account. These interactions extend over a coherence length defining a coherent unit volume, containing N particles, in which an exact electromagnetic calculation has to be performed. Our calculation is based on a recursive T-matrix algorithm [8], modified in order to avoid the convergence problems inherent to this formulation. The scattering parameters for a set of N particles are deduced from the sum of the different scattering parameters calculated for each scatterer \mathbf{k} , and expressed in an external base, the base of

the applied field:

$$\begin{aligned}
 \frac{\partial \sigma_{\text{sca}}^{\text{agg}}(\mathbf{u}_i, \mathbf{u}_j)}{\partial \Omega} &= \sum_k \frac{\partial \sigma_{\text{sca}}^k(\mathbf{u}_i, \mathbf{u}_j)}{\partial \Omega}, \sigma_{\text{sca}}^{\text{agg}}(\mathbf{u}_j) \\
 &= \sum_k \sigma_{\text{sca}}^k(\mathbf{u}_j), \sigma_{\text{ext}}^{\text{agg}}(\mathbf{u}_j) \\
 &= \sum_k \sigma_{\text{ext}}^k(\mathbf{u}_j). \tag{5}
 \end{aligned}$$

Each individual parameter depends on the individual scattered field defined by a scattering matrix $\overline{\overline{\mathbf{S}^{(k)}}}(\mathbf{u}_j, \mathbf{u}_i)$ expressed in the same external base. We calculate this matrix in two steps: (i) Addition-translation theorem [9] is invoked to calculate the individual T-matrix on the base centered on particle k , in order to account for the field scattered by a single particle k placed in an environment of $N - 1$ other scatterers; (ii) a translation gives the final expression of matrix $\overline{\overline{\mathbf{S}^{(k)}}}$ in the external base. Expressions (5) depend on the scatterers spatial configuration. The media we studied are composed with isotropically distributed scatterers. Unfortunately, there is no possibility, for the moment, to give an exact expression for the different scattering parameters averaged over all possible positions in the coherence volume. As a first approximation, we calculate these parameters for an average interparticles distance D . Another remark is that total scattering cross sections depend on the direction and polarization of the incident field. We showed [10] that scattering parameters averaged over orientations could be simply expressed as the trace of the matrix defining the cross sections (Eq. (5)) multiplied by a factor 2π .

3. Experiments

Measurements were obtained thanks to a spectro-scatterometer designed in our laboratory. It is composed with two rotating arms (Fig. 1), supporting incidence and detection optical fibers. The incidence angle is manually fixed at the beginning of each measurement session. The detection arm is motorized and has two angular movements (θ, φ). The sample is placed in a rotating plate, in order to explore all space

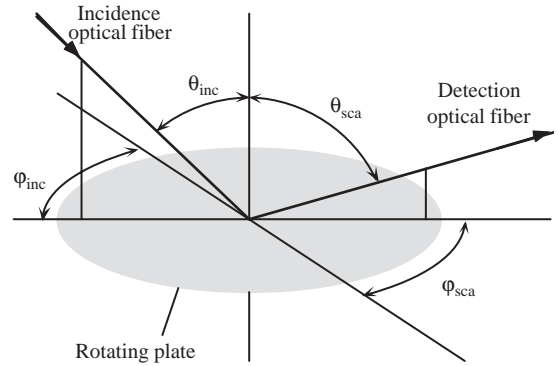


Fig. 1. Scheme of the spectro-scatterometer.

Table 1

Description of media M1 and M2. Incoherent (Mie) and coherent (AST) extinction parameters, and average interparticle distance D used for AST calculation

	M1	M2
Spheres diameter (μm)	0.1	3
Scatterers volume fraction (%)	1.5	4
Medium thickness (μm)	5000	100
D (μm)	0.23	4.2
Extinction coefficient (μm^{-1})		
Incoherent	1.963×10^{-7}	0.03357
Coherent (average)	2.410×10^{-7}	0.03167

directions. This mechanical device is coupled to a white Xenon source for illumination and an optical multichannel analyzer for detection. We consider latex beads in water as scattering elements, with gauged size in order to perform a comparison between experiments and calculations, that we placed inside silica tanks (index of refraction: $n_{\text{silica}} = 1.46$). The results are given for the wavelength $\lambda = 0.589 \mu\text{m}$, for which the index of refraction of the beads is well known: $n_{\text{latex}} = 1.59$. We give results for three cases (Table 1): (i) medium M1 (small particles); (ii) medium M2 (large particles); (iii) we couple these two media (M3), in order to give an illustration of the multilayer treatment.

4. Results and discussion

Experimental results are now compared to RTE solutions computed with incoherent (deduced from

Mie theory) and coherent (deduced from AST) scattering parameters. Assuming that main electromagnetic interactions are generally produced by interactions between two scatterers, for the considered concentrations we neglect interactions of superior orders. Average interparticles distance between scatterers D and extinction coefficients (particles are non-absorbing, $k_{\text{sca}} = k_{\text{ext}}$) for each media are given in Table 1. For M1, D is larger than two scatterer diameters and the coherent extinction coefficient, averaged over all cluster orientations, is higher than that obtained by applying Mie theory. For this case, Mie theory

underestimates the level of scattering. On the contrary, for M2, D is smaller than two diameters, and the averaged coherent extinction coefficient is weaker than the incoherent one. We plot in Fig. 2 the phase functions for M1 (a) and M2 (b). When considering incoherent calculations (gray curves), particles composing M1 behave like Rayleigh

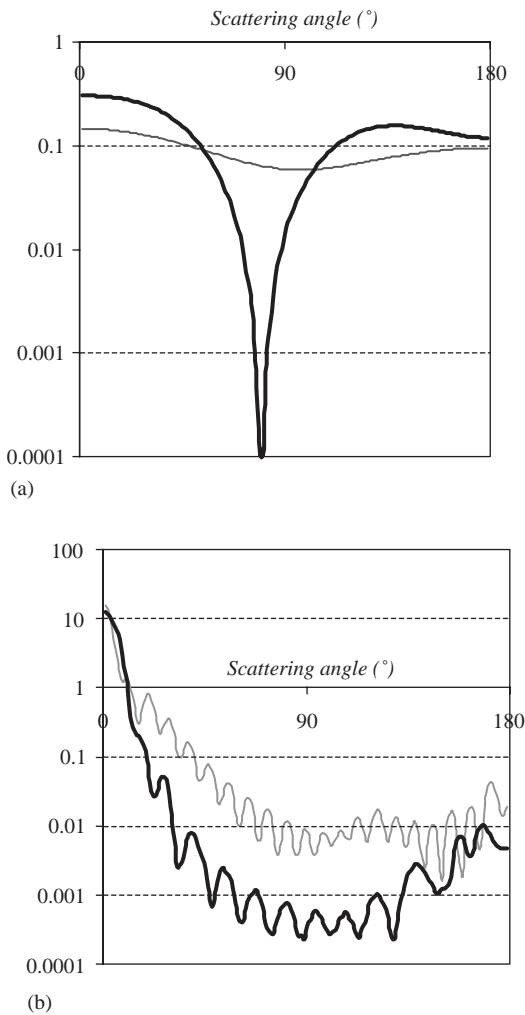


Fig. 2. Incoherent (gray curves) and coherent (black curves) phase functions for M1 (a) and M2 (b).

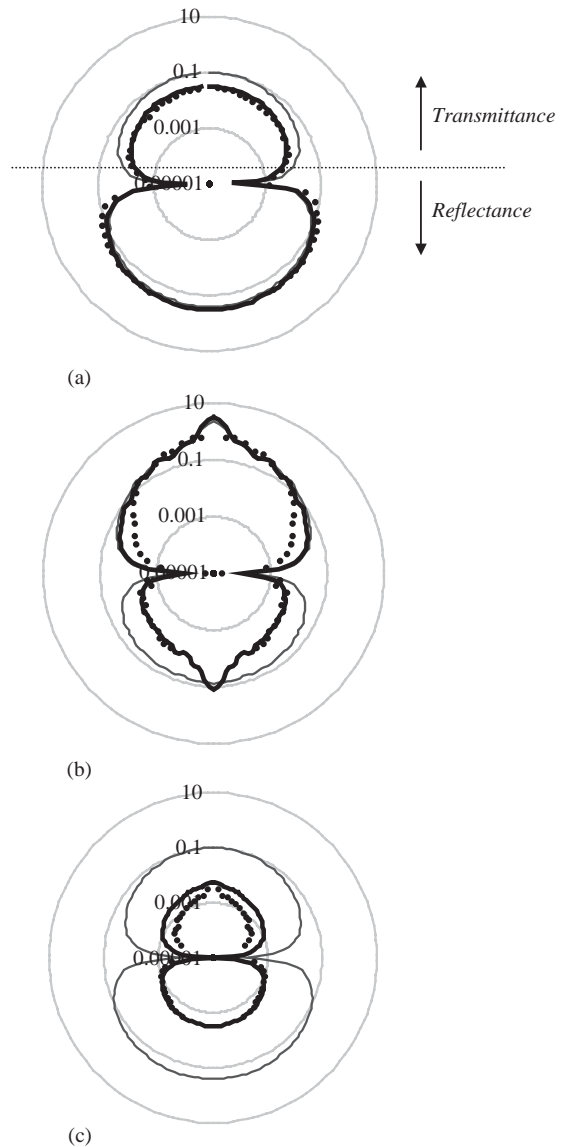


Fig. 3. Angular distribution of flux by unit solid angle for M1 (a), M2 (b) and M3 (c). Calculations (incoherent: gray curve; coherent: black curve) compared to measurements (dot curves).

scatterers, with an isotropic profile, while those of M2 behave like Mie scatterers, with a strong scattering anisotropy and the presence of multiple scattering lobes. The **coherent** calculation (black curves) enhances anisotropy and, for M2, some structures in the phase function are killed when taking into account interactions. Fig. 3 shows the angular flux distributions (plotted with logarithmic scale), expressed by unit solid angle in order to compare calculations (full curves) and experiments (dot curves). In all the cases, the **incoherent** treatment (gray curve) misestimates scattering while our **coherent** calculation (black curve) reproduces more accurately experimental results. One has nevertheless to mention few discrepancies between theoretical and experimental curves, essentially in transmission (M2 and M3). On one hand, it can be due to the approximations that we used for the calculation: (i) a more accurate calculation should be performed for the evaluation of D ; (ii) superior orders of interactions should be taken into account. On the other hand, one can

notice that this discrepancy appears when flux level is very low and the signal-to-noise ratio becomes close to 1. It can be also observed in M3 experimental curve (c) a weak anisotropy due to the presence of the Mie scattering medium.

References

- [1] S. Chandrasekhar, Radiative Transfer, Dover Publications, New York, 1960.
- [2] J.C. Auger, et al., Physica B 279 (2000) 21.
- [3] B. Stout, et al., J. Modern Opt. 48 (2001) 2105.
- [4] D.W. Mackowski, J. Opt. Soc. Am. A 11 (1994) 2851.
- [5] A. Da Silva, et al., J. Modern Opt., to appear (2003).
- [6] C.F. Bohren, D.R. Huffman, Absorption and Scattering of Light by Small Particles, Wiley-Interscience Publication, New York, 1983.
- [7] G. Mie, Ann. Phys. 25 (1908) 377.
- [8] W.C. Chew, Waves and Field in Inhomogeneous Media, IEEE PRESS Series on Electromagnetic Waves, IEEE Press, New York, 1990.
- [9] O.R. Cruzan, Quart. Appl. Math. 20 (1962) 33.
- [10] B. Stout, et al., J. Modern Opt. 49 (2002) 2129.